

Lateral Lamella of the Cribriform Plate

Software-Enabled Computed Tomographic Analysis and Its Clinical Relevance in Skull Base Surgery

C. Arturo Solares, MD; Walter T. Lee, MD; Pete S. Batra, MD; Martin J. Citardi, MD

Objective: To describe a quantitative analysis of the lateral lamella of the cribriform plate (LLCP) height in computed tomographic (CT) images. The LLCP is the thinnest anatomic structure in the skull base.

Design: Software-enabled CT scan measurements.

Setting: Academic center.

Results: The CT scans from 50 patients were analyzed. The median height of the LLCP in 100 sides was 2.4 mm. The LLCP height was 0 to 3.9 mm in 83 sides, 4.0 to 7.0 mm in 15 sides, and greater than 7.0 mm in 2 sides. When analyzing differences among sides, the LLCP height was

greater on the right side in 28 patients and greater on the left side in 22. The differences between sides was 0 to 1.9 mm in 39 patients, 2.0 to 3.9 mm in 9 patients, and greater than 4.0 mm in 2 patients.

Conclusions: Computer-aided CT scan analysis allows for a quantitative analysis of the paranasal sinus skull base anatomy. Knowledge of these dimensions is invaluable during surgical planning and navigation. Asymmetry of the relative ethmoid roof position is common. Thus, the rhinologic surgeon must exercise caution to prevent unintentional skull base injury and cerebrospinal fluid leak.

Arch Otolaryngol Head Neck Surg. 2008;134(3):285-289

THE ROOF OF THE ETHMOIDAL labyrinth is formed by the orbital plate of the frontal bone. This serves to separate the ethmoid air cells from the anterior cranial fossa. Centrally, the orbital plate articulates with the lateral lamella of the cribriform plate (LLCP). The LLCP is the thinnest anatomic structure in the skull base.¹ Because of this, it is a common site of injury to the skull base. To avoid these complications, the surgeon must have a detailed knowledge of the anatomy, which can be highly variable among patients.

Several cadaveric studies have reported the anatomic variations of the ethmoid bone.^{2,3} Keros,² in his classic study, proposed a 3-category classification based on the position of the cribriform plate (CP) relative to the ethmoid roof. More recently, computed tomographic (CT)⁴ techniques have been utilized to study ethmoid roof anatomy. Magnetic resonance imaging⁵ is considered complementary to CT because it provides soft tissue information (eg, mucocele vs meningoencephalocele) that indirectly indicates the integrity of the bony skull base. These studies highlight the anatomical variations of the

ethmoid bone and its relationship to surrounding structures.

With the advent of image-guided sinus surgery, preoperative CT review allows the surgeon to develop a 3-dimensional appreciation of relevant anatomy. Simultaneous viewing of axial, coronal, and sagittal planes and 3-dimensional model reconstruction provides the surgeon with critical anatomic information simply not afforded by static films.⁶ Previously, we applied this technology in anatomic studies of the skull base and paranasal sinuses.⁷⁻⁹ In the present report, we have used this technology to perform a quantitative analysis of LLCP height. The objectives of this study were to (1) develop a quantitative system for assessment of the LLCP, (2) measure and report LLCP height in a representative population, and (3) propose a clinically useful paradigm for the assessment of LLCP height in the era of image-guided surgery.

METHODS

The CT images were selected from a CT image archive of all patients under the care of the

Author Affiliations: Head and Neck Institute, Cleveland Clinic, Cleveland, Ohio. Dr Citardi is now with the Department of Otorhinolaryngology–Head and Neck Surgery, the University of Texas Medical School at Houston.

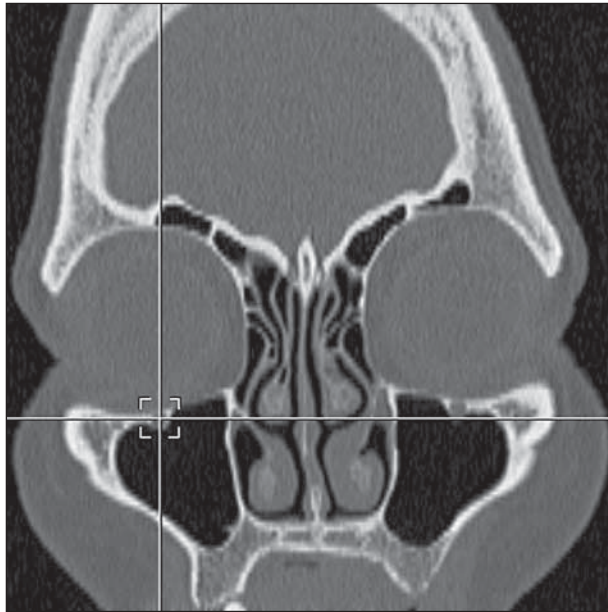


Figure 1. Coronal computed tomographic scan demonstrating the reference plane defined as the horizontal plane through the center of the infraorbital nerve.

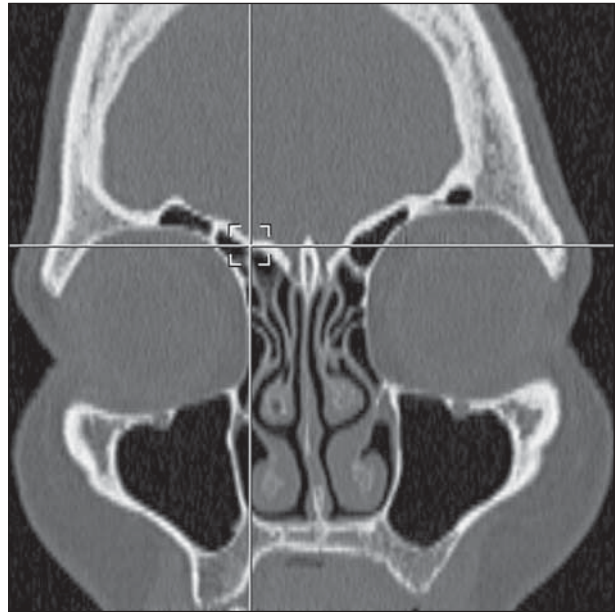


Figure 3. Coronal computed tomographic scan demonstrating the lateral ethmoid roof point defined by the intersection of a vertical line tangent to the medial orbital wall with the ethmoid roof.

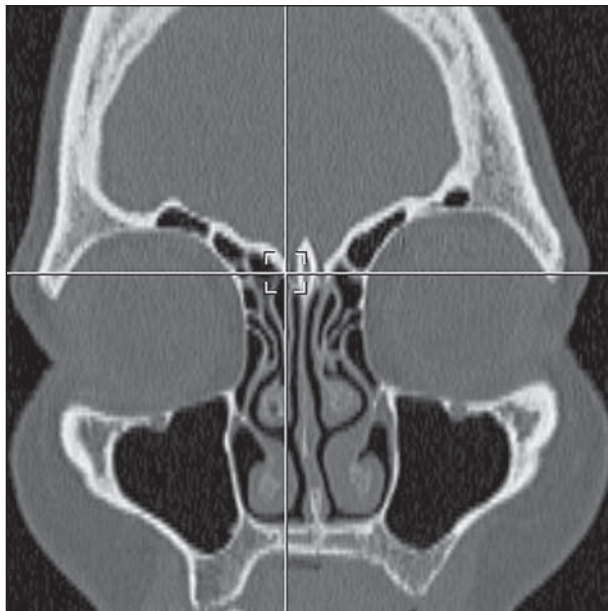


Figure 2. Coronal computed tomographic scan demonstrating the medial ethmoid roof point, defined by the articulation of the medial ethmoid roof and the lateral lamella of the cribriform plate.

senior author (M.J.C.) who had received high-resolution, 1-mm axial CT scans during 2003. Exclusion criteria included previous trauma, sinonasal tumor, sinonasal polyposis, cerebrospinal fluid leak, and notable rhinosinusitis (defined as inflammatory changes that precluded visualization of skull base anatomy). The institutional review board of the Cleveland Clinic, Cleveland, Ohio, approved the study.

All patients had undergone an axial CT scan (tube voltage, kVp 120; 100-170 mA; field of view, 125 mm; sharp or high resolution; 1.0-mm contiguous axial slice) obtained with a VolumeZoom CT scanner (Siemens, Munich, Germany). Archived images were transferred to a CBYON Suite Doctor Sta-

tion (version 2.6-2.8; Med-Surgical Services Inc, Mountain View, California) for analysis. Using the software, reconstituted sagittal and coronal images were generated. Surgical planning tools were used to measure LLCPC configuration.

For each data set, a standardized review, based on principles derived from traditional cephalometrics, was performed. This process operationally defined a method for quantifying the position of the cribriform plate and ethmoid roof relative to the orbital floor (as defined by the infraorbital nerve). The infraorbital nerve, a structure easily identified on coronal CT scan, was chosen to serve as a proxy for the orbital floor, a structure easily seen after endoscopic maxillary antrostomy (**Figure 1**). Previous work¹⁰ had demonstrated that CT image reconstructions adequately represent bony skull base anatomy.

Any CT scans in which the patient was rotated or tilted were excluded for further analysis. Three points were chosen as reference points at the skull base: the medial ethmoid roof point (MERP), which corresponded to the medial extension of the ethmoid roof (ie, its articulation with the LLCPC) (**Figure 2**); the lateral ethmoid roof point (LERP), identified by the intersection of a vertical line tangent to the medial orbital wall with the ethmoid roof (**Figure 3**); and the lowest point on the CP (**Figure 4**).

Measurements, using the distance measuring tool, were taken in the anterior plane at the first coronal cut that clearly demonstrated the CP, and in the posterior plane at the last coronal cut demonstrating the CP. The vertical distance from the MERP to the horizontal plane defined by the infraorbital nerve (termed *MERP height*), the vertical distance from the LERP to the horizontal plane defined by infraorbital nerve (termed *LERP height*), and the vertical distance from the CP to the horizontal plane defined by the infraorbital nerve (termed *CP height*) were determined (**Figure 5**). The LLCPC length was calculated by subtracting the CP height from the MERP height in the anterior and posterior planes. The lateral-medial slope of the ethmoid roof was calculated as the difference between the MERP and LERP heights in the anterior and posterior coronal planes.

Comparative calculations between sides were undertaken. In addition, clustering statistical techniques were used in an attempt to define anatomical categories for different configurations of the ethmoid roof.

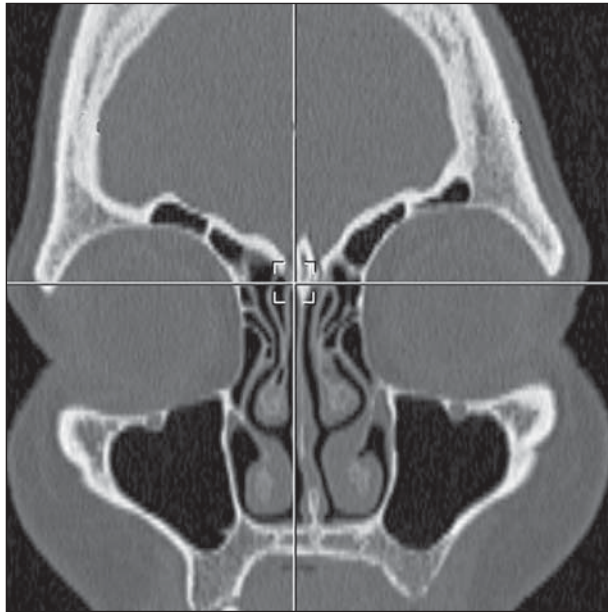


Figure 4. Coronal computed tomographic scan demonstrating the cribriform plate (CP) point identified by the lowest point of the CP.

RESULTS

The CT scans from 50 patients were analyzed. This group included 25 men and 25 women. Their mean (SD) age was 47.8 (14) years. The median height of the LLCP in 100 sides was 2.4 mm (mean [SD] height, 2.5 [1.5] mm).

Attempts to cluster patients using Euclidian and correlation coefficient clustering methods did not provide a clinically useful classification. Therefore, we categorized our data using the classic Keros classification.² The LLCP height was 0 to 3.9 mm in 83 sides, 4.0 to 7.0 mm in 15 sides, and greater than 7.0 mm in 2 sides. When analyzing differences among sides, the LLCP height was higher on the right side in 28 patients and higher on the left in 22. The difference between sides was 0 to 1.9 mm in 39 patients, 2.0 to 3.9 mm in 9 patients, and greater than 4.0 mm in 2 patients.

To characterize the configuration of the ethmoid roof in the coronal plane, the MERP height was subtracted from the LERP height. The mean (SD) difference in the anterior plane was 6.2 (2.3) mm, indicating that the LERP was on average 6.2 mm higher than the MERP. When comparing the right and left sides, this difference was greater on the left side in 27 patients and on the right side in 23 patients. In the posterior plane, the mean difference was only 3.0 (2.0) mm, indicating that the LERP was on average 3.0 mm higher than the MERP. Intriguingly, in 6 sides the MERP was higher than the LERP in the posterior plane.

Representative CT images for relevant skull base anatomy are presented (**Figures 6, 7, and 8**).

COMMENT

The present study provides a quantitative analysis of the ethmoid roof position and configuration. Using computer-aided CT scan analysis, we were able to measure reliably the ethmoid roof height and determine the LLCP

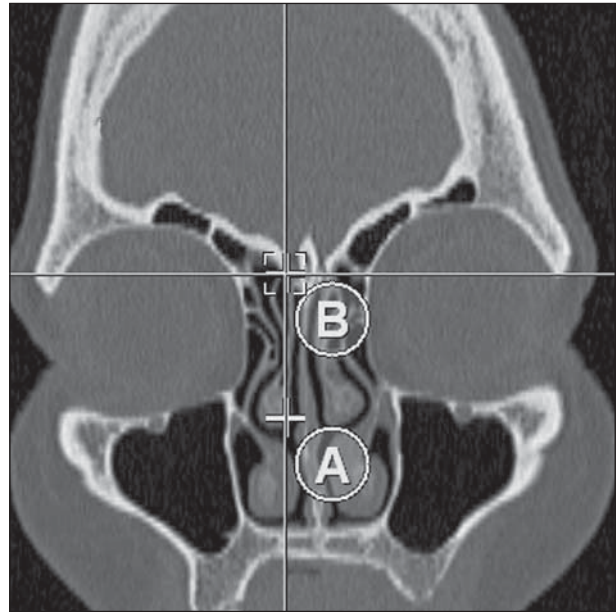


Figure 5. Coronal computed tomographic scan demonstrating the use of navigation tools to measure the vertical distance from the medial ethmoid roof point (MERP) to the horizontal plane defined by the infraorbital nerve (termed *MERP height*). (In this instance, the software's distance-measuring tool determined the distance between point A [the reference plane] and point B [the MERP, in this instance]. The vertical distance from the lateral ethmoid roof point [LERP] to the horizontal plane defined by the infraorbital nerve [termed *LERP height*] and the vertical distance from the cribriform plate [CP] to the horizontal plane defined by the infraorbital nerve [termed *CP height*] were determined in a similar manner.)

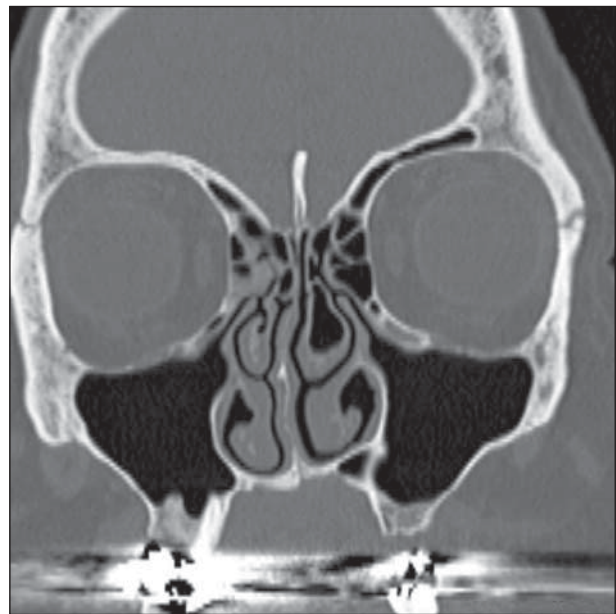


Figure 6. Coronal computed tomographic (CT) scan demonstrating a symmetric, "short" cribriform plate (CP) lateral lamella (CPLL). In this CT scan, the difference between the medial ethmoid roof point height and CP height is nearly zero, but the lateral ethmoid roof point height is greater. Measurements are similar on each side. These quantitative measurements summarize the relevant skull base anatomy; that is, the CPLL is short, the lateral ethmoid roof is high, and both sides share similar anatomic features.

height. Knowledge of these dimensions is invaluable to avoid injury to the skull base, particularly at its most vulnerable structure, the LLCP. In this patient population,



Figure 7. Coronal computed tomographic scan demonstrating an asymmetric, “tall” cribriform plate (CP) lateral lamella. In this instance, the difference between the medial ethmoid roof point (MERP) height and the CP height is greater than 4.0 mm, and the measurement is similar on each side. Furthermore, the MERP and lateral ethmoid roof point heights are greater on the left side compared with the right side; that is, these values capture the qualitative observation of CP and ethmoid roof asymmetry.

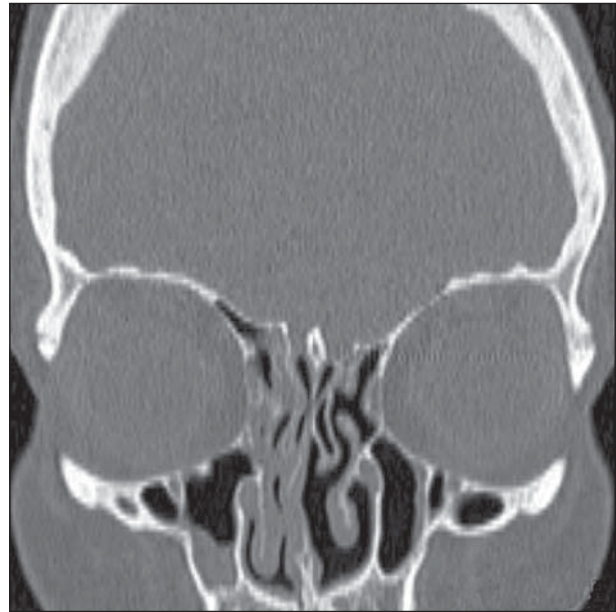


Figure 8. Coronal computed tomographic scan demonstrating an asymmetric cribriform plate (CP) and ethmoid roof. In this instance, the right medial ethmoid roof point and lateral ethmoid roof point heights are greater than the corresponding values on the left side, and the CP lateral lamella height is also greater on the right side.

considerable intersubject anatomical variation was observed; therefore, the surgeon had to carefully review the patient’s anatomy on the preoperative CT scan prior to performing surgery. Surgical navigation tools, such as the one described herein, may be utilized to analyze the anatomy prior to surgery.

Previous anatomical studies have attempted to classify the different configurations of the ethmoid roof. Keros² proposed a 3-category classification based on height of the LLCP according to the analysis of 450 skulls. In the first type, the olfactory groove was 1 to 3 mm deep. This type occurred in 12% of the specimens studied by Keros.² In the current series, all LLCP heights of less than 4 mm were grouped together; this first group included 83% of sides. The second type comprised all the cases in which the CP was located 4 to 7 mm under the ethmoid roof and occurred in 70% of the specimens studied by Keros.² In the current series of patients, this occurred in 15% of sides. The third type occurred in 18% of Keros’s specimens and comprised cases in which the CP was 8 to 16 mm deeper than the roof of the ethmoid. In the current series of patients, this configuration was noted in only 2% of sides. The reasons for the apparent differences in the prevalences of the various LLCP height groups are difficult to determine. One cannot discount real differences in the populations under study. Furthermore, differences in technique (cadaveric dissection vs computer-aided CT review) may influence the apparent measurements. Finally, in the current study, all LLCP heights of less than 4 mm were grouped together; this definition is more inclusive than the class I definition offered by Keros² (1-3 mm).

As the height of the LLCP increases, the possibility of penetrating the skull base increases. In addition, Jang

et al¹¹ found a direct correlation between the height and the incidence of dehiscences in the LLCP on coronal CT imaging. The differences in the distribution of skull base configurations between our study and Keros’s original study² highlight the high anatomical variability in this region. Thus, knowledge of the LLCP configuration is important during ethmoid surgery, which makes the preoperative imaging review a must.

The current study also presents additional information about the configuration of the ethmoid roof. In the anterior coronal plane the ethmoid roof is lower medially at its articulation with the LLCP. It rises from medial to lateral in a “gull wing” configuration.¹² In the current series of patients, the lateral ethmoid roof was consistently higher than the medial ethmoid roof in the anterior coronal plane. However, posteriorly, 6% of sides were noted to have an “inverted” configuration (ie, a higher medial height). This suggests that the ethmoid roof at the posterior skull base becomes flatter. Furthermore, the anterior ethmoid roof (at the MERP) was consistently higher at the anterior coronal plane.

In regard to the configuration of the ethmoid roof, when comparing sides, asymmetry is typically found (Figure 7 and Figure 8). The LLCP height was higher on the right side in 56% of patients. However, the LERP was higher than the MERP on the left side in 54% of patients. Dessi et al¹³ reported that the ethmoid roof was asymmetric in about 10% of their cases, whereas Lebowitz et al¹² reported asymmetries of the ethmoid roof in 57% of their patients. In our patient population, asymmetries were noted in all subjects. Perhaps this is due to the use of computer-aided CT scan analysis, which allows for more accurate measurements of the skull base.

Zacharek et al¹⁴ also used computer-aided CT scan analysis to study the ethmoid roof. These investigators performed bilateral measurements on 100 consecutive sinus CT scans. They noted that there was considerable variability at the anterior ethmoid roof. However, the posterior ethmoid roof in their study showed minimal variability. This relative “flattening” of the ethmoid roof posteriorly was also noted in the current study. These investigators¹⁴ chose the palate as their inferior reference point.

All measurements were determined relative to the floor of the orbit at the infraorbital nerve. This landmark is easily identified after endoscopic maxillary antrostomy, and thus a surgeon may estimate the ethmoid roof position by visualization alone by using this landmark as a reference point. In this paradigm, LLC height, and so forth, are measured on the CT; this information may then be used to guide visual estimates obtained under endoscopic visualization. More important, relative positions of the MERP, LERP, and CP, which together define the configuration of the ethmoid roof, may be studied on the preoperative imaging (Figures 6, 7, and 8), and during surgery, their positions relative to the orbital floor may be estimated. In this way, information that may be critical for the avoidance of skull base injury may be applied easily during surgery. For surgeons who use surgical navigation, the strategy for assessing the ethmoid roof configuration employed in this report may also be utilized during preoperative planning and then applied during intraoperative surgical navigation.

In conclusion, in this study, a computer-aided surgery system was used to review archived CT scans to perform a quantitative analysis of the ethmoid roof position and configuration. The relative positions of the ethmoid roof and CP were determined, and then distance measuring tools in the computer software were used to characterize these positions. This approach quantitatively defines the configuration of the LLC height. The described paradigm may be useful during preoperative review of digital CT scan images and during intraoperative surgical navigation. Thus, the paradigm serves to facilitate understanding of skull base anatomy in the era of image-guided surgery.

Submitted for Publication: August 15, 2006; final revision received August 5, 2007; accepted August 28, 2007.

Correspondence: Martin J. Citardi, MD, Department of Otorhinolaryngology–Head and Neck Surgery, University of Texas Medical School at Houston, 6431 Fannin, MSB 5.202, Houston, TX 77030 (martin.j.citardi@uth.tmc.edu).

Author Contributions: Drs Solares, Lee, Batra, and Citardi had full access to all the data in the study and take responsibility for the integrity of the data and the accu-

racy of the data analysis. *Study concept and design:* Solares, Lee, Batra, and Citardi. *Acquisition of data:* Solares and Lee. *Analysis and interpretation of data:* Solares, Batra, and Citardi. *Drafting of the manuscript:* Solares, Batra, and Citardi. *Critical revision of the manuscript for important intellectual content:* Solares, Lee, Batra, and Citardi. *Administrative, technical, and material support:* Lee and Citardi. *Study supervision:* Lee, Batra, and Citardi.

Financial Disclosure: Dr Citardi was a member of the scientific advisory board of CBYON from 1999 to 2003. He currently is a member of the scientific advisory board of GE Healthcare Navigation and Visualization.

Previous Presentation: This study was presented in part at the 2006 Triologic Society Annual Meeting; May 21–22, 2006; Chicago, Illinois.

REFERENCES

1. Terrier F, Weber W, Ruefenacht D, Porcellini B. Anatomy of the ethmoid: CT, endoscopic and macroscopic. *AJR Am J Roentgenol.* 1985;144(3):493-500.
2. Keros P. On the practical value of differences in the level of the lamina cribrosa of the ethmoid [in German]. *Z Laryngol Rhinol Otol Ihre Grenzgeb.* 1962;41:808-813.
3. Schmidt HM. Über masse und niveaudifferenzen der medianstrukturen der vorderen Schädeldelgrube des Menschen. *Gegenbaurs Morphol Jahrb.* 1974;120:538-539.
4. Bolger WE, Butzin CA, Parsons DS. Paranasal sinus bony anatomic variations and mucosal abnormalities: CT analysis for endoscopic sinus surgery. *Laryngoscope.* 1991;101(1, pt 1):56-64.
5. Kraus DH, Lanzieri CF, Wanamaker HR, Little JR, Lavertu P. Complementary use of computed tomography and magnetic resonance imaging in assessing skull base lesions. *Laryngoscope.* 1992;102(6):623-629.
6. Citardi MJ, Batra PS. Image-guided sinus surgery: current concepts and technology. *Otolaryngol Clin North Am.* 2005;38(3):439-452.
7. Batra PS, Citardi MJ, Gallivan RP, et al. Software-enabled computed tomography analysis of the carotid artery and sphenoid sinus pneumatization patterns. *Am J Rhinol.* 2004;18(4):203-208.
8. Batra PS, Citardi MJ, Gallivan RP, et al. Software-enabled CT analysis of optic nerve positioning and paranasal sinus pneumatization patterns. *Otolaryngol Head Neck Surg.* 2004;131(6):940-945.
9. Citardi MJ, Gallivan RP, Batra PS, et al. Quantitative computer-aided computed tomography analysis of sphenoid sinus anatomical relationships. *Am J Rhinol.* 2004;18(3):173-178.
10. Citardi MJ, Herrmann B, Hollenbeak CS, Stack BC, Cooper M, Buchholz RD. Comparison of scientific calipers and computer-enabled CT review for the measurement of skull base and craniomaxillofacial dimensions. *Skull Base.* 2001;11(1):5-11.
11. Jang YJ, Park HM, Kim HG. The radiographic incidence of bony defects in the lateral lamella of the cribriform plate. *Clin Otolaryngol Allied Sci.* 1999;24(5):440-442.
12. Lebowitz RA, Terk A, Jacobs JB, Holliday RA. Asymmetry of the ethmoid roof: analysis using coronal computed tomography. *Laryngoscope.* 2001;111(12):2122-2124.
13. Dessi P, Moulin G, Triglia JM, Zanaret M, Cannoni M. Differences in the height of the right and left ethmoid roofs: a possible risk factor for ethmoidal surgery: prospective study of 150 scans. *J Laryngol Otol.* 1994;108(3):261-262.
14. Zacharek MA, Han JK, Allen R, et al. Sagittal and coronal dimensions of the ethmoid roof: a radioanatomic study. *Am J Rhinol.* 2005;19(4):348-352.